Optimizing Coupled Two-Agent Motion in the Plane

Kyle Fitzgerald (with April Roszkowksi)

Advisor: Andy Borum, Cornell University Department of Mathematics

Funding: ELI Undergraduate Research Funds

August 19, 2019

Abstract

In this report, we analyze an optimal control problem involving the coupled motion of two agents moving in a plane. The agents' motion is required to locally minimize a cost function that penalizes the curvature of each agent's path as well as the difference between their path curvatures. The weight placed on the curvature difference term in the cost function determines the strength of coupling between the agents' motion. Conditions necessary for optimality are from the Pontryagin Maximum Principle, while conditions sufficient for optimality are from conjugate point theory. Via numerical solutions, we discover a vast space of bifurcations that exists between solutions with zero coupling, where agents act individually, and solutions with infinite coupling, where agents explicitly mimic each other. These bifurcations generally indicate changes in solution optimality, meaning that a solution transitions from locally minimizing the cost function to extremizing it in a different way. This leads us to conclude that most extremal trajectories only solve the optimal control problem for finite ranges of coupling. This is a problem of interest in the context of swarm mechanics and is a step towards modeling various kinds of neighbor-influenced behavior in animals.

1 Introduction

The study of optimal collective motion investigates the dynamic behavior of a group of agents whose goal is to achieve an objective while minimizing an accumulated cost function. Perhaps the most frequently-investigated problem in optimal collective motion is that of energy minimization during locomotion. Here, the objective is for each agent to move from a start point to an end destination, and the cost function to be minimized is that of accumulated energy expenditure.

We are interested in how individual and group behavior are affected when agents are influenced by each other's actions, or *coupled*. This broadly describes many real-world phenomena. For example, in the near future, one may wish to achieve surgical precision with a swarm of cell-sized robots whose goal is to navigate the bloodstream to remove a tumor [1] [2]. Each individual's motion will depend in some way on the trajectories of its neighbors. Another example is *allelomimesis*, which describes animals' tendency to mimic each other's behavior (including feeding, reacting to danger, etc.) [3].[1]

The specific problem we investigate involves two agents moving in a plane. Each agent is nonholonomically constrained to move forward with unit speed and cannot instantaneously move in the lateral direction. The turning rate of agent i, i.e. the curvature of the agent's path, is given by u_i. We let (x_1, x_2) denote the position of the first agent in the plane and we let x_3 denote the orientation of its forward direction relative to the x_1 direction. Figure 1 shows a schematic of the coordinates describing the agent's configuration. Similarly, we let (x_4, x_5) denote the position of the second agent in the plane and we let x_6 denote the orientation of its forward direction relative to the x_1 direction. The coordinates describing the agents' configurations and turning rates are related by the differential equations

$$\begin{bmatrix} \dot{x_1} \\ \dot{x_2} \\ \dot{x_3} \end{bmatrix} = \begin{bmatrix} \cos x_3 \\ \sin x_3 \\ u_1 \end{bmatrix}, \quad \begin{bmatrix} \dot{x_4} \\ \dot{x_5} \\ \dot{x_6} \end{bmatrix} = \begin{bmatrix} \cos x_6 \\ \sin x_6 \\ u_2 \end{bmatrix}. \tag{1}$$

We specifically require that each agent moves from the origin to the point $(0.5, 0)$ in the plane, and that each agent begins and ends facing the x_1 direction. This provides a symmetry between agent boundary conditions that can be exploited to generate a set of "canonical" agent paths. These requirements correspond to the following boundary conditions:

$$\mathbf{x}(t=0) = \begin{bmatrix} 0 & 0 & 0 & 0 & 0 & 0 \end{bmatrix}^T, \quad \mathbf{x}(t=1) = \begin{bmatrix} 0.5 & 0 & 0 & 0.5 & 0 & 0 \end{bmatrix}^T \tag{2}$$

Finally, we define a cost function that penalizes the curvature of each agent's path as well as the difference between their path curvatures, where the magnitude of a parameter $\mu \in \mathbb{R}_{\geq 0}$ determines the strength of the coupling between the agents. This is achieved with the cost function

$$g(u_1, u_2, \mu) = \frac{1}{2}\left(u_1(t)^2 + u_2(t)^2 + \mu\left(u_1(t) - u_2(t)\right)^2\right) \tag{3}$$

[1] In this report, we will focus on determining a collective optimal behavior rather than assigning optimal response behaviors to each individual at each time step. This is akin to designing an overarching control mechanism for robots or modeling a deep-rooted evolutionary mechanism in animals, rather than allowing for individual autonomy.

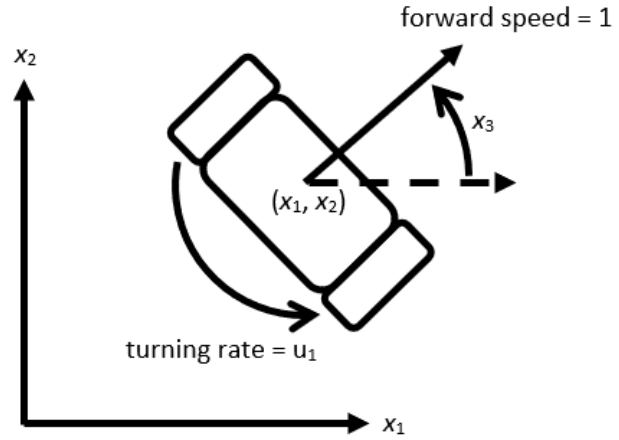

Figure 1: Schematic of agent 1 in the optimal control problem. Agent 2 is described by coordinates $\{x_4, x_5, x_6\}$ and turning rate u_2.

Putting all of this together yields the full optimal control problem:

$$\begin{aligned} &\min_{\mathbf{x},\, u_1,\, u_2} \ \frac{1}{2}\int_0^1 u_1(t)^2 + u_2(t)^2 + \mu\,(u_1(t) - u_2(t))^2\, dt \\ &\text{s.t.} \quad \begin{bmatrix} \dot{x_1} \\ \dot{x_2} \\ \dot{x_3} \end{bmatrix} = \begin{bmatrix} \cos x_3 \\ \sin x_3 \\ u_1 \end{bmatrix}, \quad \begin{bmatrix} \dot{x_4} \\ \dot{x_5} \\ \dot{x_6} \end{bmatrix} = \begin{bmatrix} \cos x_6 \\ \sin x_6 \\ u_2 \end{bmatrix}, \\ &\mathbf{x}(0) = \begin{bmatrix} 0 & 0 & 0 & 0 & 0 & 0 \end{bmatrix}^T, \quad \mathbf{x}(1) = \begin{bmatrix} 0.5 & 0 & 0 & 0.5 & 0 & 0 \end{bmatrix}^T \end{aligned} \tag{4}$$

The two coupling extremes, i.e. zero coupling (which simplifies the motion to two single-agent optimality problems) and infinite coupling (which dictates that agents follow paths that resemble each other as much as possible) have been investigated analytically by Justh and Krishnaprasad [4]. They found that solutions to the former can be expressed in terms of Jacobi elliptic functions. They also found that the *average* of the agents' positions in the latter problem behaves just like a single-agent problem and can thus also be written in terms of Jacobi elliptic functions. However, little was said about cases with finite coupling. Additionally, the authors only analyzed the necessary conditions for optimality, which merely guarantees that solutions extremize the cost function without ensuring that they minimize it.

In this paper, we use numerical methods to solve the optimal control problem with finite coupling. The Pontryagin Maximum Principle is used to find solutions that extremize the cost function [5] and results from conjugate point theory are used to determine whether the solutions obtained are indeed optimal or, instead, some other non-minimal extremum [6].

For our particular boundary value problem (BVP), we build up a solution-space diagram that contains various bifurcations, at each of which there is a change in the number of conjugate points in the solution trajectories. To do this, we first establish a set of "canonical" single-agent paths that solve the problem for zero coupling. We then combine these paths in various ways to create zero-coupling solutions for two agents. Finally, we determine the effect of slowly increasing the coupling on each path combination and plot the results.

2 Hamiltonian Dynamics and Conjugate Point Theory

2.1 A General Optimal Control Problem

Let us start with an example. Given the optimal control problem

$$\begin{aligned} &\min_{\mathbf{x},\,\mathbf{u}} \int_0^T g(\mathbf{x}(t),\mathbf{u}(t))\,dt, \\ &\text{s.t.} \quad \dot{\mathbf{x}}(t) = f(\mathbf{x}(t),\mathbf{u}(t))\,, \\ &\mathbf{x}(0) = \mathbf{x_0}, \quad \mathbf{x}(T) = \mathbf{x_T}, \end{aligned} \tag{5}$$

where $\mathbf{x} \in \mathbb{R}^n$ and $\mathbf{u} \in \mathbb{R}^m$, we first determine the necessary conditions for optimality using the Pontryagin Maximum Principle [5]. We define the system's Hamiltonian to be

$$H(\mathbf{p},\mathbf{x},\mathbf{u}) = \mathbf{p}\cdot f(\mathbf{x},\mathbf{u}) - g(\mathbf{x},\mathbf{u}), \tag{6}$$

where $\mathbf{p}$ is the costate vector and is analogous to a Lagrange multiplier in finite-dimensional optimization. The state vector $\mathbf{x}$ and the costate vector $\mathbf{p}$ obey Hamilton's canonical equations, giving us a system of $2n$ ordinary differential equations:

$$\dot{\mathbf{x}} = \frac{\partial H}{\partial \mathbf{p}}, \quad \dot{\mathbf{p}} = -\frac{\partial H}{\partial \mathbf{x}}, \tag{7}$$

Additionally, for the control input $\mathbf{u}$ to be optimal, it must maximize H at all times. That is,

$$\mathbf{u}(t) = \arg\max_{\mathbf{v}\in\mathbb{R}^m} H(\mathbf{p}(t),\mathbf{x}(t),\mathbf{v}) \quad \forall\, t \in [0,T] \tag{8}$$

We then determine the sufficient conditions for optimality using conjugate point theory [6]. We must solve the matrix differential equation

$$\begin{bmatrix}\dot{M}\\ \dot{J}\end{bmatrix} = A\begin{bmatrix}M\\ J\end{bmatrix}, \qquad A(t) = \begin{bmatrix} -\dfrac{\partial^2 H}{\partial \mathbf{p}\partial \mathbf{x}} & -\dfrac{\partial^2 H}{\partial \mathbf{x}^2} \\ \dfrac{\partial^2 H}{\partial \mathbf{p}^2} & \dfrac{\partial^2 H}{\partial \mathbf{x}\partial \mathbf{p}} \end{bmatrix}, \tag{9}$$

where $M(t), J(t) \in \mathbb{R}^{n\times n}$; $M(0) = I$; $J(0) = 0$; and $A(t) \in \mathbb{R}^{2n\times 2n}$. A solution is optimal if $\det J(t) \neq 0$ for all $t \in (0,1)$. Any time $t \in (0,1)$ where $\det J(t) = 0$ indicates a suboptimal solution and is called a *conjugate point*. (The test is inconclusive if $t = 1$ is the only conjugate point.) If a conjugate point exists in this interval, then there exists a direction of trajectory deformation such that a lower-energy configuration is achieved.

2.2 Analytical Methods for Two Coupled Agents

The Hamiltonian for our problem is as follows:

$$\begin{aligned} H(\mathbf{p},\mathbf{x},u_1,u_2) &= \mathbf{p}\cdot\dot{\mathbf{x}} - \left(\frac{u_1(t)^2}{2} + \frac{u_2(t)^2}{2} + \frac{\mu}{2}\left(u_1(t)-u_2(t)\right)^2\right) \\ &= p_1\cos x_3 + p_2 \sin x_3 + p_3 u_1 + p_4 \cos x_6 + p_5 \sin x_6 + p_6 u_2 \\ &\qquad - \frac{u_1(t)^2}{2} - \frac{u_2(t)^2}{2} - \frac{\mu}{2}\left(u_1(t)-u_2(t)\right)^2. \end{aligned} \tag{10}$$

We apply Hamilton's canonical equations from equation (7) and obtain the equations of motion

$$\begin{bmatrix} \dot{x_1} \\ \dot{x_2} \\ \dot{x_3} \\ \dot{x_4} \\ \dot{x_5} \\ \dot{x_6} \end{bmatrix} = \begin{bmatrix} \cos x_3 \\ \sin x_3 \\ u_1 \\ \cos x_6 \\ \sin x_6 \\ u_2 \end{bmatrix}, \quad \begin{bmatrix} \dot{p_1} \\ \dot{p_2} \\ \dot{p_3} \\ \dot{p_4} \\ \dot{p_5} \\ \dot{p_6} \end{bmatrix} = \begin{bmatrix} 0 \\ 0 \\ p_1 \sin x_3 - p_2 \cos x_3 \\ 0 \\ 0 \\ p_4 \sin x_6 - p_5 \cos x_6 \end{bmatrix}. \tag{11}$$

We obtain an extremal solution to our problem if the Hamiltonian is maximized for $t \in [0, T]$, i.e. the u-gradient of H is the zero vector:

$$\nabla_u H = \begin{bmatrix} p_3 - u_1 - \mu(u_1 - u_2) \\ p_6 - u_2 - \mu(u_2 - u_1) \end{bmatrix} = \begin{bmatrix} 0 \\ 0 \end{bmatrix} \tag{12}$$

This is solved by the following controls:

$$u_1 = \frac{1}{2\mu + 1}\big((1 + \mu)p_3 + \mu p_6\big), \quad u_2 = \frac{1}{2\mu + 1}\big(\mu p_3 + (1 + \mu)p_6\big) \tag{13}$$

One can verify that these control values do indeed maximize H by showing that the Hessian of H is negative definite.

To sufficiently determine the optimality of a solution, we refer to equation (9). The coupled two-agent problem has $M, J \in \mathbb{R}^{6\times 6}$ and $A \in \mathbb{R}^{12\times 12}$ with A sparse, defined by

$$\begin{aligned} \frac{\partial^2 H}{\partial \mathbf{x}^2} &= \big(-p_1 \cos x_3 - p_2 \sin x_3\big)\delta_{x_3 x_3} + \big(-p_4 \cos x_6 - p_5 \sin x_6\big)\delta_{x_6 x_6}, \\ \frac{\partial^2 H}{\partial \mathbf{p}^2} &= \frac{\mu + 1}{2\mu + 1}\big(\delta_{p_3 p_3} + \delta_{p_6 p_6}\big) + \frac{\mu}{2\mu + 1}\big(\delta_{p_3 p_6} + \delta_{p_6 p_3}\big), \\ \frac{\partial^2 H}{\partial \mathbf{x} \partial \mathbf{p}} &= -\delta_{p_1 x_3} \sin x_3 + \delta_{p_2 x_3} \cos x_3 - \delta_{p_4 x_6} \sin x_6 + \delta_{p_5 x_6} \cos x_6, \\ \frac{\partial^2 H}{\partial \mathbf{p} \partial \mathbf{x}} &= \left(\frac{\partial^2 H}{\partial \mathbf{x} \partial \mathbf{p}}\right)^T, \end{aligned} \tag{14}$$

where δ_{ij} is the matrix element in the i^{th} row and j^{th} column of the corresponding second-derivative matrix.

2.3 Numerical Methods

2.3.1 Solving the BVP

The dynamical constraints in equation (11) constitute a second-order system of differential equations with the Dirichlet boundary conditions given in equation (2). Because we have Dirichlet boundary conditions, we must employ a "shooting" method to solve the BVP. It fixes the endpoint $\mathbf{x}(0)$ and iteratively solves initial value problems (IVPs) in order to compute increasingly-accurate guesses for the initial canonical momentum $\mathbf{p}(0)$ that places the second endpoint at the boundary condition $\mathbf{x}(1)$. Specifically, we solve the IVP given in equation (9) with boundary condition $\mathbf{x}(0)$ and initial guess $\mathbf{p}(0)$, generate an error vector

$\mathbf{e}$ that points from the current value for $\mathbf{x}(1)$ to the desired value for $\mathbf{x}(1)$, and solve the matrix equation

$$J(1) \cdot \mathbf{dp_0} = -\mathbf{e}, \tag{15}$$

where $J(1)$ is the Jacobian of $\mathbf{x}(1)$ with respect to $\mathbf{p}(0)$, computed in equation (9). This allows $\mathbf{p}(0)$ to effectively descend the gradient towards the desired boundary condition. The IVP is then solved again with initial momentum $\mathbf{p}(0) + \mathbf{dp_0}$, and this process is iterated until $||\mathbf{e}||_2 < 10^{-6}$.

2.3.2 Detecting Conjugate Points

Recall that a conjugate point $t \in (0, 1)$ indicates that a solution is suboptimal. In order to detect a conjugate point once a solution is obtained, we compute $\det J(t)$ for all $t \in (0, 1)$. Numerically, determining the existence of a conjugate point corresponds to finding that $|\det J(t)| < \epsilon$, where ϵ is a small chosen tolerance. This presents a problem, as the initial condition $J(0) = 0$ means that $|\det J(\delta)| < \epsilon$ for small enough δ, which would falsely numerically indicate a conjugate point at $t = \delta$. This prompts us to ensure that $|\det J(t)|$ first increases beyond ϵ for small values of t before a conjugate point can be detected.

3 Bifurcations in $\mathbf{p}(0)$-Space

With the aforementioned numerical methods, different solutions can be obtained from different initial guesses for $\mathbf{p}(0)$. We make an attempt to organize these by first establishing the three basic "canonical" forms (shown in figure 2) that solve the single-agent problem when there is zero coupling.

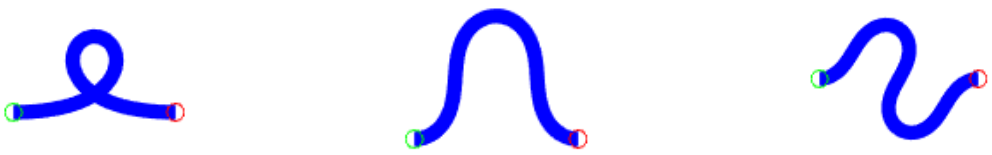

(a) Loop (b) Bell (c) S-shape

Figure 2: The three canonical single-agent trajectories in the plane for zero coupling. They are distinguished by number of inflections points: the loop has zero, the bell has two, and the S-shape has three. The loop and bell have no conjugate points, meaning they are optimal, while the S-shape has a conjugate point and is thus suboptimal.

For zero coupling, we can combine all permutations of these trajectories (as well as their reflections over the x_1/x_4-axis and the x_2/x_5-axis) to solve the two-agent problem. Also solutions to the problem are "concatenations" of these canonical forms, e.g. trajectories with multiple loops or additional inflection points in the bell, the latter of which is shown in figure 3.

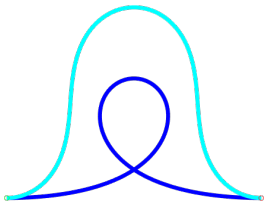

(a) Bell and Loop

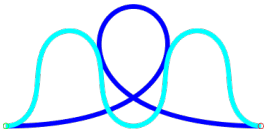

(b) Double Bell and Loop

Figure 3: Two examples of two-agent trajectories for zero coupling generated by combining/reflecting/concatenating the canonical paths in figure 2. The cyan trajectory in (b) has two concatenated bells.

Once coupling is introduced, we are no longer able to describe the complete set of solutions, as trajectories deform in a less-predictable manner. Solutions are generated via perturbations to the coupling; that is, given a solution $\mathbf{p}(0)$ for a given μ, we use $\mathbf{p}(0)$ as a guess for the initial momentum that solves the BVP for a small change in coupling $\mu + \Delta\mu$. Noteworthy is the nature in which optimality changes as coupling increases, such as that shown in figure 4.

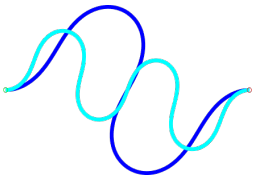

(a) Downward S, Downward Double-S: $\mu = 0$

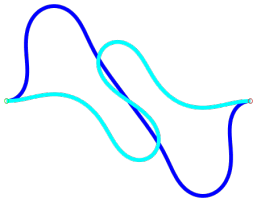

(b) Downward S, Downward Double-S: $\mu = 1.47$

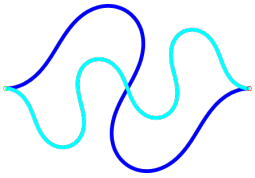

(c) Downward S, Upward Double-S: $\mu = 0$

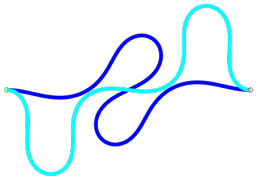

(d) Downward S, Upward Double-S: $\mu = 0.82$

Figure 4: Figures (b) and (d) are generated by taking the zero-coupling paths in figures (a) and (c) and continuously increasing coupling via small perturbations. Notice that even solutions that look similar under zero coupling can deform quite differently when coupling is introduced. (a)-(b) The "downward S, downward double-S" solution is optimal from $\mu = 0.95$ to at least $\mu = 2$. (c)-(d) The "downward S, upward double-S" solution is only optimal for $\mu \in [0.81, 0.84]$.

Given that each solution is associated with a unique value of $\mathbf{p}(0)$, points were plotted in $\mathbf{p}(0)$-space as solutions were generated in an attempt to gain further insight. As this was done, an intricate bifurcation structure emerged.

In figure 5a, we see a subcritical pitchfork bifurcation, which has an optimal branch that splits into three single-conjugate point branches, and mirror instances of supercritical pitchfork bifurcations, each of which has a two-conjugate point branch that splits into

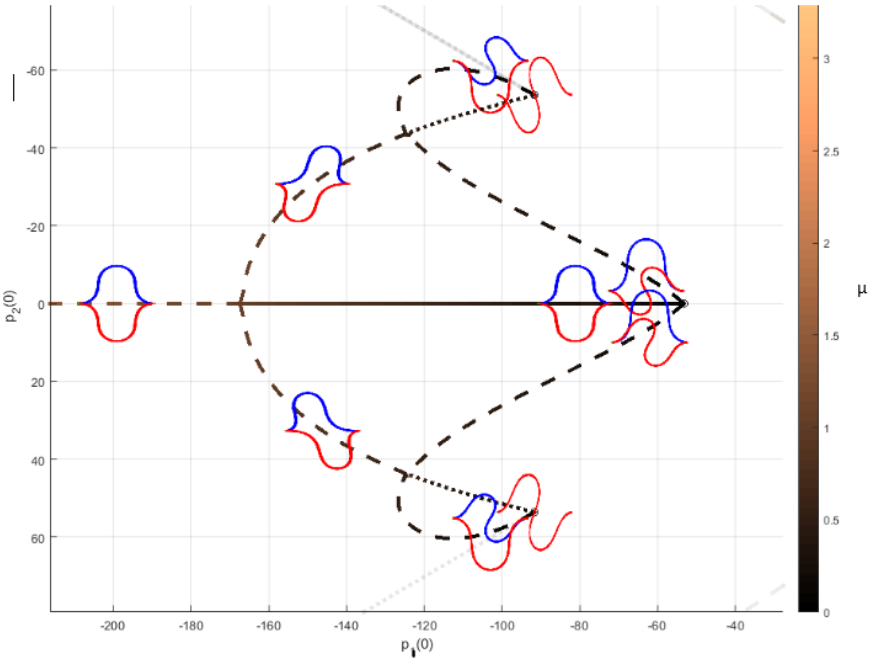

(a) A tree with bell and S-trajectories

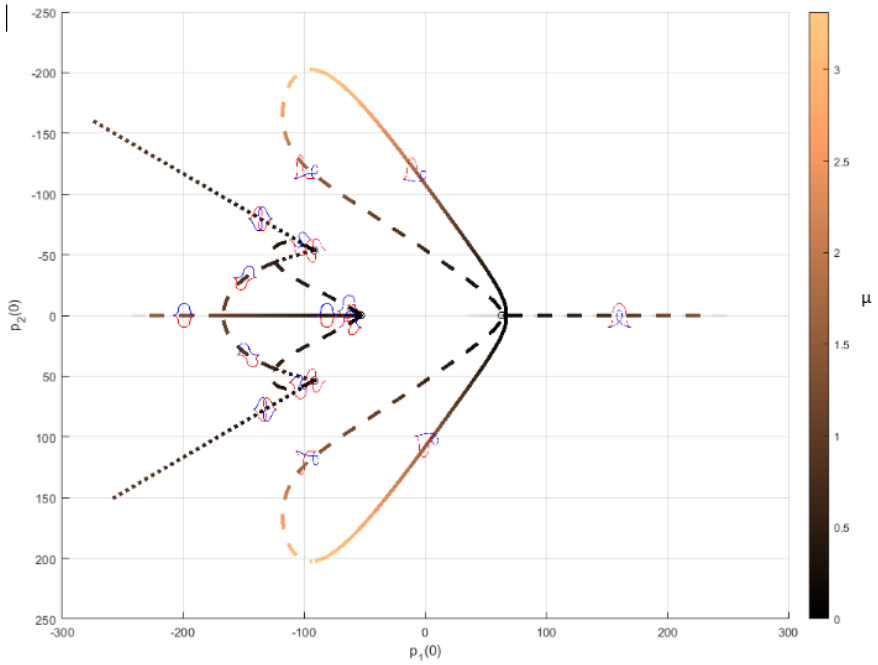

(b) A zoomed-out view of (a) containing a tree with loop trajectories

Figure 5: Two views of a partial $\mathbf{p}(0)$-space bifurcation diagram that plots the change in $p_1(0)$ and $p_2(0)$ with the coupling μ. Corresponding agent trajectories overlay the $\mathbf{p}(0)$-space diagram, with $p_1(0)$ and $p_2(0)$ from the *blue* trajectories. Solid lines denote optimal solutions, dashed lines denote suboptimal solutions with one conjugate point, and dotted lines denote suboptimal solutions with ≥ 2 conjugate points.

three single-conjugate point branches. This solution "tree" clearly presents the topological equivalence of the bell and S-shape, as changing the coupling can deform a bell into an S-shape and vice versa.[2]

In figure 5b, on the right-hand solution tree, we see a supercritical pitchfork bifurcation whose arms each contain the annihilation of an optimal solution and a single-conjugate point solution at a saddle-node bifurcation. Note that this tree is separate from the one in 5a because the plotted momenta correspond to loop trajectories in the plane, which are topologically distinct from bell and S-trajectories.

4 Discussion and Conclusions

A rich bifurcation structure with respect to coupling strength exists for the optimal control problem in which the coupled path curvatures of two agents confined to the plane are minimized, as previously outlined. This is as one would expect, given that the transitions between optimality and suboptimality are analogous to transitions between stability and instability in traditional bifurcation analysis.

While the 2+1−dimensional (momentum+coupling) diagram in figure 5 gives a nice visualization of some of the bifurcations that arise, it should be noted that not all intersections are actually intersections (or thus bifurcations) in the full 6+1−dimensional solution space. This is why we see intersections at places with equivalent blue agent trajectories but distinct red agent trajectories, e.g. near $(p_1(0), p_2(0)) = (-50, 0)$.

Note that the full bifurcation diagram has an infinite number of solution trees. This is because one can continue to construct solutions for zero coupling ad infinitum via concatenation – for example, one agent can traverse an arbitrary number of loops. None of the $\mathbf{p}(0)$-space trees corresponding to arbitrary-loop trajectories would connect to each other or to the trees in figure 5 because the trajectories are topologically distinct.

One might also mistakenly suspect an infinite number of branches to be generated by bifurcations. However, this cannot be true. Recall that infinite coupling, with these boundary conditions, forces agents to traverse the same path. This implies the existence of bifurcations that annihilate branches at larger coupling values, leaving only those that correspond to perfectly-overlaying agent paths. We suspect that many of the bifurcations between paths involving bells and S-shapes will be pitchforks, given that these paths can smoothly deform into one another, while the bifurcations between paths involving topologically inequivalent structures will be saddle-nodes, given that a loop *cannot* deform into a bell, an S-shape, or a different number of loops while fixing the endpoints.

Interestingly, as previously noted, seemingly-small changes to paths can affect optimality significantly. Perhaps the best example of this that we have come across is the comparison between an "upward loop, upward bell" (ULUB) trajectory and an "upward loop, downward bell" (ULDB) trajectory (see figure 6). The ULUB is optimal only for coupling values $\mu \in [0, 0.03]$; after this, it maintains a single conjugate point through at least $\mu = 3$. On the other hand, the ULDB is optimal for at least $\mu \in [0, 1000]$. In fact, we have not yet found the value at which the ULDB loses optimality, though we know it must exist because the

[2]To be clear, a "branch" is a line in $\mathbf{p}(0)$-space whose endpoints are bifurcations, and a "tree" is a collection of connected branches.

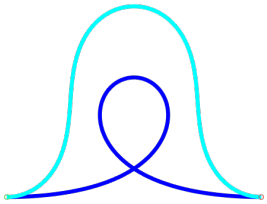

(a) Upward Loop, Upward Bell (ULUB)

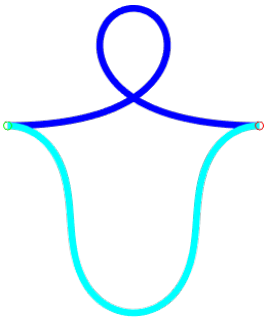

(b) Upward Loop, Downward Bell (ULDB)

Figure 6: Two examples of two-agent trajectories for zero coupling whose only difference is a reflection across the x_1-axis, but whose optimality behavior under coupling differ tremendously.

loop cannot deform into a bell in order to solve the BVP for infinite coupling.

On a related note, while some solutions are optimal for small coupling and lose optimality as coupling increases, many other solutions are *only* optimal once there is a finite amount of coupling. Consider the "downward S, downward double-S" trajectory in figure 4, which is suboptimal for $\mu \in [0, 1.47]$, beyond which it becomes optimal.

Of course, the above results apply only to one set of boundary conditions, which were chosen because requiring that paths have the same endpoint and end trajectory allowed us to easily visualize the canonical forms described earlier. More work is required to investigate problems with boundary conditions that do not exhibit this nice simplification.

Analytically characterizing the solutions for all boundary conditions appears to be challenging. However, we may be able to study certain families of solutions. In particular, we intend to explore a family characterized by $p_1 = p_2 = p_4 = p_5 = 0$, thus requiring $p_3 = C_1$, $p_6 = C_2$, referring to equation (11). Qualitatively, this limits us to solutions with constant curvature, i.e. circles.

5 References

[1] Galstyan, A., Hogg, T., & Lerman, K. (2005, August). Modeling and mathematical analysis of swarms of microscopic robots. *Proceedings 2005 IEEE Swarm Intelligence Symposium*. (doi:10.1109/SIS.2005.1501623)

[2] Hogg, T. (2007). Coordinating microscopic robots in viscous fluids. *Auton Agent Multi-Agent Systems* **14**: 271. (https://doi.org/10.1007/s10458-006-9004-3)

[3] Juanico, D. E., Monterola, C., & Saloma, C. (2005, April). Cluster formation by allelomimesis in real-world complex adaptive systems. *Phys. Rev. E* **71**: 041905. (https://doi.org/10.1103/PhysRevE.71.041905)

[4] Justh, E. W. & Krishnaprasad, P. S. (2015, March). Optimality, reduction and collective motion. *Proc. R. Soc. A* **471**: 20140606. (https://doi.org/10.1098/rspa.2014.0606)

[5] Pontryagin, L. S., Boltyanskii, V. G., Gamkrelidze, R. V., & Mishchenko, E. F. (1962). *The Mathematical Theory of Optimal Processes*. New York, NY: Wiley.

[6] Agrachev, A. A. & Sachkov, Y. L. (2004). *Control Theory from the Geometric Viewpoint*. Berlin, Germany: Springer.